Systems & Control Transactions

Research Article - Peer Reviewed Conference Proceeding
ESCAPE 35 - European Symposium on Computer Aided Process Engineering
Ghent, Belgium. 6-9 July 2025
Jan F.M. Van Impe, Grégoire Léonard, Satyajeet S. Bhonsale,
Monika E. Polańska, Filip Logist (Eds.)

PSE PRESS

Optimal Design and Analysis of Thermochemical Storage and Release of Hydrogen via the Reversible Redox of Iron Oxide/Iron

Richard Yentumi[a,b], Constantin Jurischka[a], Bogdan Dorneanu[a], and Harvey Arellano-Garcia[a]*

[a] FG Prozess-und Anlagentechnik, Brandenburgische Technische Universität, Cottbus, Germany
[b] Department of Engineering & Maintenance, Ghana National Gas Company (GNGC), Accra, Greater Accra, Ghana
* Corresponding Author: arellano@b-tu.de

ABSTRACT

In this contribution, a thermodynamic model-based approach for the optimal design of a solid-state hydrogen storage and release system utilizing the reversible iron oxide/iron thermochemical redox mechanism is presented. Existing storage processes using this mechanism face significant limitations, including low hydrogen conversion, high energy input requirements, limited storage density, and slow charging/discharging kinetics. To address these challenges, a custom thermodynamic model using NIST thermochemistry data is developed, enabling an in-depth analysis of redox reaction equilibria under different conditions. Unlike previous studies, this approach integrates a multi-objective optimization framework that explicitly balances competing objectives: maximizing hydrogen yield while minimizing thermal energy demand. By systematically identifying optimal trade-offs, the study provides new insights into improving process efficiency and reactor design for thermochemical hydrogen storage. These findings contribute to advancing energy-efficient and scalable hydrogen storage technologies.

Keywords: Hydrogen, Hydrogen Fuel Cells, Energy Storage, Modelling and Simulations, Optimisation, Thermochemical storage, Green hydrogen

INTRODUCTION

As the European Union (EU) aims to reach net zero emissions by 2050, green hydrogen (H_2) has emerged as a clean alternative to existing mainstream hydrocarbon fuels and even unabated hydrogen. One of the major challenges with hydrogen, however, is that it is relatively difficult to store at large scale. Moreover, gaseous and liquefied hydrogen storage processes are energy intensive and expensive [1]. More recently, there has been growing interest in the development of cost-effective and energy-efficient solid-state processes for hydrogen storage. Thermochemical storage (TCS) is emerging as a promising method. As defined by De Rosa et al. [2], thermochemical storage is any storage method based on reversible chemical reactions in which heat is stored and released during the forward endothermic and reverse exothermic reactions respectively. The principle behind thermochemical hydrogen storage is the reversible reduction and oxidation of a metal oxide/pure metal pair. The balanced chemical equation for this reaction is written as:

$$Fe_3O_4\,(s) + 4H_2\,(g) \rightleftharpoons 3Fe\,(s) + 4H_2O\,(g)$$

In the forward endothermic reaction, the solid metal oxide (Fe_3O_4) is reduced to a pure metal (Fe) with hydrogen acting as the reducing agent. The hydrogen feed is thus converted to steam. In the reverse exothermic reaction, the pure metal (Fe) is re-oxidised to a metal oxide (Fe_3O_4) with water/steam acting as the oxidising agent. Essentially, hydrogen is stored in the reduction reaction and the metal oxide acts a solid-state storage medium. The stored hydrogen may be recovered in the reverse oxidation reaction. Figure 1 shows the schematic of a thermochemical storage system.

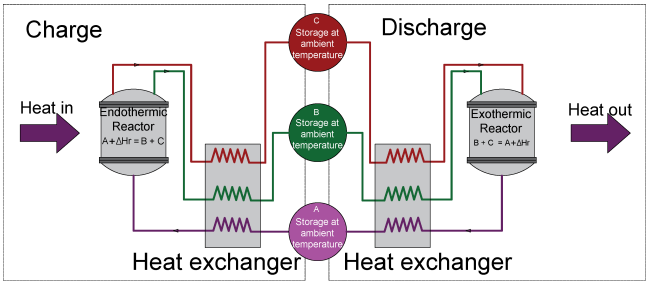

Figure 1. Schematic of a thermochemical storage system

To underscore the suitability Fe_3O_4/Fe pair, Brinkman et al. [3] evaluated various other metal oxide/pure metal candidate pairs such as ZnO/Zn, SnO_2/Sn, GeO_2/Ge, $WO_{2.722}$/W, MoO_2/Mo, for use as solid-state storage mediums for hydrogen. Considering evaluation criteria such as process conditions, energy requirements, material costs, and storage density, they identified Fe_3O_4/Fe as the optimal candidate pair. However, it is important to note that Otsuka et al. [4] were the first to propose this storage method for hydrogen fuel cell vehicles (FCVs). Brinkman et al. [3] highlighted that the strict performance requirements - such as energy density, process conditions, and charging/discharging response times - make it unlikely that this cyclical storage method will adequately meet the demands of FCV applications. Conversely, they suggested that for large-scale, long-term storage applications, where cost and safety are the primary concerns, the hydrogen TCS method could serve as a viable alternative.

From this perspective, chemical reactor design, a vital step in the development of hydrogen TCS processes, is the overall aim of this work. Different reactor types being studied include fixed bed or fluidised bed reactors.

In this contribution, Section 2 presents a novel fixed-bed single reactor concept. Additionally, it outlines a custom thermodynamic model developed using the NIST Standard Reference Database 69: *NIST Chemistry WebBook* [5] and details its model-based optimisation. Section 3 presents and discusses the results. Finally, conclusions are drawn in Section 4.

2. METHODOLOGY

2.1 Single-Reactor Concept

Most research on hydrogen TCS has been carried out based on a two-reactor system (Figure 1) – an endothermic reactor for reduction and an exothermic reactor for oxidation [3]. To maximise energy efficiency, such systems include heat exchangers and other equipment units. Thus, overall, the CAPEX and OPEX outlays for these systems are high. Thus, a fixed bed type single reactor concept is proposed that combines the endothermic and exothermic reactors into a single unit with the primary aim of minimising energy input through heat integration. The proposed concept consists of four main operating modes that include: standby/factory mode; storage process; cold storage mode; and release process. Figure 2 illustrates the proposed operating modes.

In *standby mode*, the outer shell of the reactor is packed with beds of Fe while the inner shell is packed with beds of Fe_3O_4. In the *storage process*, a green hydrogen feed which is available to be stored, flows into the inner shell for reduction of the metal oxide while steam is introduced into the outer shell to oxidise the pure metal into a metal oxide. A portion of the thermal energy released from the exothermic oxidation reaction in the outer shell meets the heat input requirements of the endothermic reduction reaction in the inner shell. Once almost all the pure gaseous products of hydrogen from the outer shell and the steam from the inner shell are removed, the storage process completes, and the unit may be allowed to cool down and enter a *cold storage mode* which theoretically may be long term durations. It is important to note that once the storage process is complete, the outer shell shall consist of beds of Fe_3O_4 while the inner shell contains Fe. To initiate the hydrogen *release mode*, on-site hydrogen is fed to the outer shell for reduction of Fe_3O_4 to Fe while steam is fed to the inner shell for oxidation of Fe to Fe_3O_4. A portion of the thermal energy released from this exothermic oxidation reaction thus, feeds the endothermic reaction in the outer shell. The net effect of these alternating redox reactions in the outer and inner shells results in the minimisation of the overall energy input required for hydrogen TCS.

Moreover, besides the comparative advantage of lower costs, this proposal offers several other advantages such as the potential for miniaturisation for mobile applications such as in FCVs. Some potential challenges with this concept may include maintainability problems, challenges with its dynamic operations nature, temperature controllability challenges, heat transfer management between shells, special high temperature materials requirement, and so on.

2.2 Thermodynamic Model

The objective of the proposed model is to predict the reaction temperature that maximises equilibrium conversion. Integration of thermodynamic and chemical reaction equilibrium yields this powerful model; to predict the reaction equilibrium constant and other key thermodynamic physical properties (temperature, pressure, etc.) as well as thermodynamic functions such as enthalpy, entropy and Gibbs free energy of the reacting system. This algebraic thermochemical equilibrium model is given as:

$$\Delta_r G^o(T) = -RT\ ln\ K_{eq} \quad (1)$$

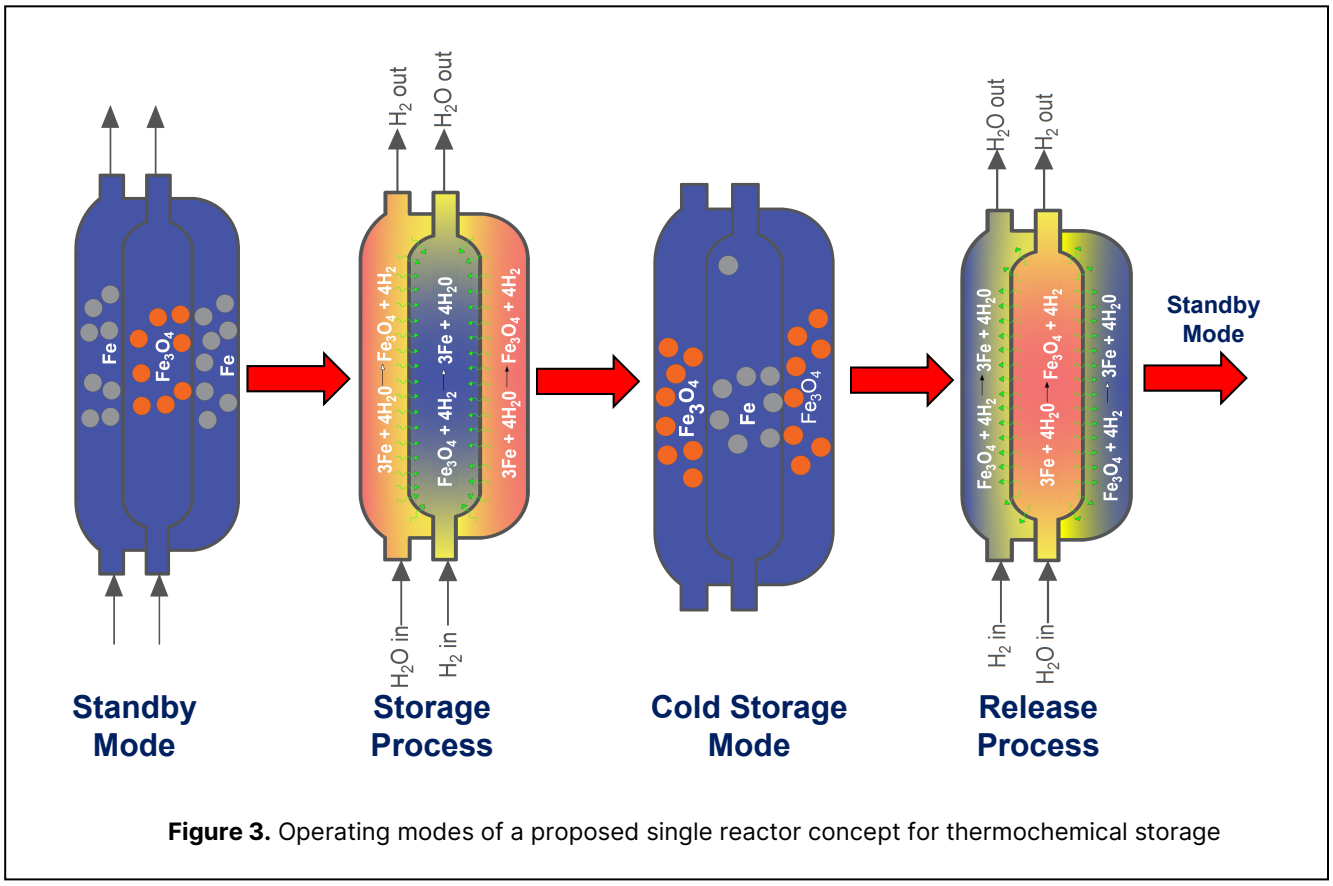

Figure 3. Operating modes of a proposed single reactor concept for thermochemical storage

The standard change in Gibbs free energy, $\Delta_r G^o$, at a fixed temperature and pressure is estimated from the relation:

$$\Delta_r G^o(T) = \Delta_r {H_f}^o - T\Delta_r S^o \qquad (2)$$

From the NIST Thermochemistry data [5], the magnitude of the standard enthalpy change of a reaction $\Delta_r H_f^o$ is the sum of the standard enthalpies of formation of the products, each multiplied by its appropriate coefficient, minus the sum of the standard enthalpies of formation of the reactants, also multiplied by their coefficients. The standard entropy change of a reaction, $\Delta_r S^o$, is estimated similarly. The equilibrium constant as a function of the reaction temperature, T, for each reaction is estimated from the relation:

$$K_{eq}(\mathrm{T}) = exp^{\left(-\frac{\Delta_r G^o(T)}{RT}\right)} \qquad (3)$$

Brinkman et al. [3] reported that under the idealisations similarly applied for this work, varying the reactor pressure had no significant effect on equilibrium conversion (x).

The equilibrium conversion (x) in dimensionless units and as a function of temperature is thus, estimated as follows:

$$x_{H_2}(\mathrm{T}) = \left(\frac{SC_{H_2}}{SC_{H_2O}}\right) \cdot \frac{\left[K_{eq}(\mathrm{T}).q_{n,H_{2-in}}\right]}{\left[q_{n,H_{2-in}} + K_{eq}(\mathrm{T}).q_{n,H_{2-in}}\right]} \qquad (4)$$

$$x_{H_2O}(\mathrm{T}) = \left(\frac{SC_{H_2O}}{SC_{H_2}}\right) \cdot \frac{\left[K_{eq}(T).q_{n,H_2O-in}\right]}{\left[q_{n,H_2O-in} + K_{eq}(T).q_{n,H_2O-in}\right]} \qquad (5)$$

Where SC is the stoichiometric coefficient (dimensionless); $K_{eq}(T)$is equilibrium constant (dimensionless) and $q_{n,}$ is molar flow rate (kmol/hr). The heat flow for the forward reduction reaction, $Q_f(T)$ and that for the reverse oxidation reaction, $Q_r(T)$, both in kW, are estimated from the relations.

$$Q_f(\mathrm{T}) = Q_{products}(\mathrm{T}) - Q_{reactants}(T) \qquad (6)$$

$$Q_r(\mathrm{T}) = Q_{products}(\mathrm{T}) - Q_{reactants}(T) \qquad (7)$$

Where the heat flow for the products or reactants may be determined from the relation:

$$Q_i = \sum_{i=1}^{n} q_{n,i} \cdot \Delta {h_i}^o(T) \qquad (8)$$

Where n is the number of chemical components. The total enthalpy in kJ/kmol of the reactant and product streams are estimated from the relation:

$$\Delta h^o(\mathrm{T}) = \sum y_i \cdot \left[{h_{f,i}}^o + h^o(T)\right] \tag{9}$$

The temperature dependent enthalpies $h^o(T)$ for each chemical component are estimated from the component specific NIST thermochemistry data heat capacity (Shomate equation).

2.3 Optimisation Model

The purpose of the optimisation study is to identify optimal operating conditions in the presence of trade-offs between conflicting objectives; maximisation of equilibrium conversion and minimisation of energy input in both the reduction and oxidation processes. The presence of these conflicting objectives gives rise to a multi-objective optimisation problem (MOOP).

Eq. (10) shows the general structure of a MOOP for the forward reduction reaction with the reaction temperature, T, as the decision variable.

Equation (1) sets thermodynamic boundaries on the total energy changes occurring during the reactions. Equation (2) establishes feasibility limits on the composition of the reaction system at equilibrium.

The decision variable, T, was constrained to operate within a range of 25°C and bounded at approximately 80% of the melting point temperature of iron (Fe) reported by [6]. In practical terms, this helps prevent melting and other forms of physical degradation of the solid particles, such as sintering, agglomeration, and so on.

MOOP differs from a single objective optimisation problem (SOOP), in that two or more objective functions are required to be solved within the specified constraints simultaneously. Moreover, whereas a unique optimal solution may exist for SOOPs, a set of trade-off solutions may typically exist for MOOPs.

$$\begin{gathered} max \;\; f_1(T) = x_{\mathrm{H2}}(T) \\ min \;\; f_2(T) = Q_f(T) \\ s.t. \\ Eqn.(1) \\ Eqn.(3) \\ T^{LB} \leq T \leq T^{UB} \end{gathered} \tag{10}$$

Several methods currently exist for solving MOOPs. The epsilon(ε)-constrained method (ECM) first proposed by Haimes et al. [7] was applied in this study as it yields the set of exact Pareto-optimal solutions efficiently. In applying the ECM, a so-called primary objective function is selected to be optimised while the other remaining objective functions are converted into constraints with predefined upper bounds ε_i. The ε_i-values were selected based on industrial-scale constraints to guarantee feasible solutions.

Notwithstanding, it is essential to highlight that all objectives hold the same level of importance, in that, no weights of preference are assigned to the objective functions as with some other methods. However, in general, the successful implementation of ECM requires careful specification of feasible ε_i values and consideration of computational efficiency.

In the reduction step, equilibrium conversion of hydrogen was specified as the primary objective function in the description of the MOOP in ECM form as shown in Eq. (11).

$$\begin{gathered} min \;\; -f_1(T) = -x_{\mathrm{H_2}}(T) \\ s.t. \\ f_2(T) = Q_f(T) \leq \varepsilon \\ Eqn.(1) \\ Eqn.(3) \\ T^{LB} \leq T_f \leq T^{UB} \end{gathered} \tag{11}$$

Similarly, the ECM form for the reverse oxidation reaction is shown in Eq. (12):

$$\begin{gathered} min \;\; -f_1(T) = -x_{\mathrm{H_2O}}(T) \\ s.t. \\ f_2(T) = Q_r(T) \leq \varepsilon \\ Eqn.(1) \\ Eqn.(3) \\ T^{LB} \leq T_r \leq T^{UB} \end{gathered} \tag{12}$$

The gradient-based MATLAB nonlinear solver fmincon was used to solve the resulting SOOPs within the practical bounds of the decision variable (reaction temperature) and by systematically varying the constraints which includes the ε_i values.

The results generated from solving the MOOP is a set of non-dominated or Pareto-optimal solutions of the entire feasible decision space. The superiority of the final solution (best compromised solution) over the other solutions is determined by the decision-maker mostly based on a combination of technical and economic considerations.

In this work, the fuzzy based method as proposed by Yalcin & Erginel [8] was used to identify the best compromised solutions out of the set of Pareto efficient solutions for each of the objective functions. For each reaction, the optimum is a set of solutions that define the best trade-off between the competing maximisation (Eq. 13)

and minimisation (Eq. 14) objective functions.

$$\mu_k(T) = \frac{f_k(T) - f_k^*}{f_k^* - f_k'} \quad (13)$$

$$\mu_k(T) = \frac{f_k' - f_k(T)}{f_k' - f_k^*} \quad (14)$$

Maximum and minimum values of the maximization and minimisation objectives are calculated from Eqs. (15) and (16) under the problem constraints, respectively.

$$f_k^* = max\big(f_k(T)\big), \quad f_k' = min\big(f_k(T)\big) \quad (15)$$

$$f_k^* = min\big(f_k(T)\big), \quad f_k' = max\big(f_k(T)\big) \quad (16)$$

The best compromised solution being the first solution point with the largest numerical value for $\mu_k(T)$.

3. RESULTS & DISCUSSION

Figure 3 shows a plot of the model predicted equilibrium conversion vs. reaction temperature for the reduction (red curve) and the oxidation (blue) curves.

The reduction step is favoured by high temperatures; equilibrium conversion of hydrogen in the range $0.50 \leq x_{H_2} \leq 0.9999$ were predicted to occur within operating temperature range of $792\ K \leq T_f \leq 1307\ K$, respectively.

Conversely, the oxidation step is favoured by lower temperatures; such that within similar equilibrium conversion bounds for steam (x_{H_2O}), the predicted temperature range is $792\ K \leq T_r \leq 568\ K$, respectively.

Although the results suggest that conducting the reduction step at high temperatures enhances conversion rates, it is essential to account for the drawbacks of high operating temperatures, including safety risks, increased energy consumption, higher costs, and other related factors. Moreover, Spreitzer and Schenk [9] have reported, referencing the Baur-Glassner diagram, that at reduction temperatures > 570 °C, Fe_3O_4 is first reduced to wüstite (an intermediate oxide) before being further reduced to pure Fe. While the chemical thermodynamic effects of wüstite formation was ignored in this work, it may be important to characterise its overall effect on the model.

To identify optimum operating conditions for the redox reactions, Pareto front diagrams, the boundary marked out by the set of all points plotted from the Pareto-optimal set were developed.

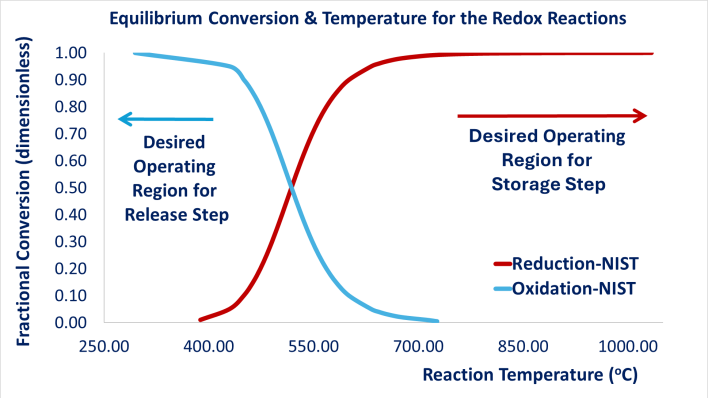

Figure 3. Equilibrium equilibrium conversion vs temperature of the redox reactions

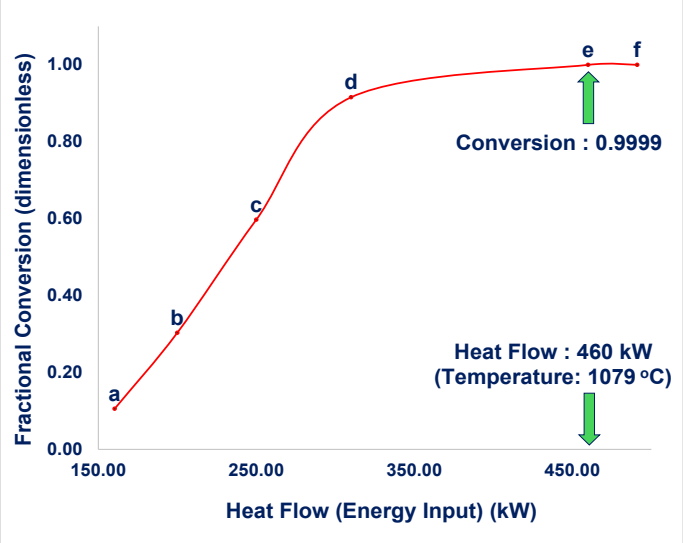

Figure 4. Pareto front diagram showing the best compromised solution for reduction

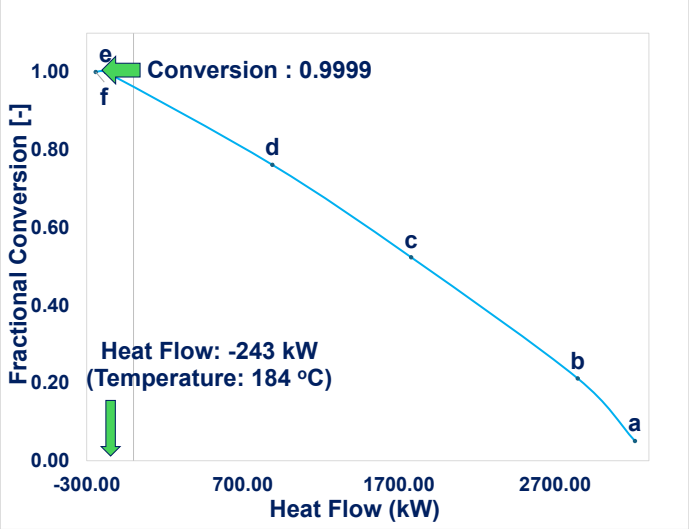

Figure 5. Pareto front diagram showing best compromised solution for oxidation

Figure 4 shows the Pareto front considering heat flow (energy input) and equilibrium conversion for the endothermic forward reduction reaction, while Figure 5 illustrates the Pareto front considering heat flow and equilibrium conversion for the exothermic reverse oxidation reaction.

Furthermore, the best compromised solutions for the endothermic reduction and exothermic oxidation reactions were determined and spot-lighted in Figures 4 and 5, respectively, using the fuzzy-based method.

Overall, the results obtained show that for once-through process storage step, reduction should be conducted at a temperature of about 1079 °C while oxidation for the release step should be conducted at about 184 °C. The results obtained also show potential for energy savings owing to configuration of the single reactor concept through heat integration.

As highlighted by Smith [10], it is important to note that the predicted equilibrium conversion values are independent of the reactor design and represent the absolute maximum conversions of reactants in a reversible reaction mixture at a given temperature and pressure.

4. CONCLUSIONS

In this work, the thermo-chemical feasibility of a reactor concept for hydrogen storage and release has been established. Through thermodynamic modeling and optimization, ideal operating conditions have been identified, maximizing hydrogen conversion while minimizing energy input. The proposed reactor concept demonstrates the potential for significantly lower specific energy requirements compared to conventional compressed and liquefied hydrogen storage methods, offering a promising alternative for efficient hydrogen storage.

To further refine the system, detailed kinetic studies using the shrinking core model have been conducted to determine lab-scale charging and discharging times. Ongoing experimental work is focused on assessing the long-term stability of the Fe_3O_4/Fe system and exploring performance enhancements through the incorporation of metal oxide/metal pairs as structural supports.

Future work includes the development of a dynamic distributed parameter model to capture spatial and temporal variations within the reactor. Further efforts will focus on improving energy efficiency, optimizing key performance metrics, and advancing the scalability of this storage technology for practical applications.

ACKNOWLEDGEMENTS

The project has been funded by Bundesministerium für Wirtschaft und Klimaschutz (BMWK) under grant number 03EI3102C. The authors would also like to thank the CEO of GNGC, Ben K.D Asante, PhD, for his visionary investments in this research work.

REFERENCES

1. Raman R, Nair VK, Prakash V, Patwardhan A, Nedungadi P, Green-hydrogen research: What have we achieved, and where are we going? Bibliometrics analysis, *Energy Reports*, 8, 9242–9260 (2022)
2. De Rosa M, Afanasevab O, Fedyukhinc AV, Bianco V, Prospects and characteristics of thermal and electrochemical energy storage systems, *Journal of Energy Storage*, 44, 103443 (2021)
3. Brinkman L, Bulfin B, Steinfeld A, Thermochemical hydrogen storage via the reversible reduction and oxidation of metal oxides, *Energy Fuels*, 35, 18756-18767 (2021)
4. Otsuka K, Yamada C, Kaburagi T, Takenaka S, Hydrogen storage and production by redox of iron oxide for polymer electrolyte fuel cell vehicles, *International Journal of Hydrogen Energy*, 28, 335-342 (2003)
5. NIST Chemistry WebBook, SRD 69 (webpage), https://webbook.nist.gov/chemistry/
   Condensed Phase Thermochemistry Data for: Fe_3O_4 and Fe.
   Gas Phase Thermochemistry Data for H_2 and H_2O.
6. Desai P.D, Thermodynamic properties of iron and silicon, *Journal of Physical and Chemical Reference Data*, 15, 967-983 (1986)
7. Haimes Y, Lasdon L, Wismer D, On a bicriterion formulation of the problems of integrated system identification and system optimization, *IEEE Transactions on Systems, Man, and Cybernetics*, 1:296-297 (1971)
8. Yalcin GD, Erginel N, Determining weights in multi-objective linear programming under fuzziness, *World Congress on Engineering*, Vol II (2011)
9. Spreitzer D, Schenk J, Reduction of iron oxides with hydrogen—A review, *Steel Research Int.*, 90,1900108 (2019)
10. Smith R, Chemical Process Design and Integration, 2nd Edition, John Wiley & Sons Ltd (2016)